







Automated Assessment of Cell Infiltration and Removal in Decellularized Scaffolds – Experimental Study in Rabbits

Avaliação automatizada da infiltração e remoção celular em scaffolds descelularizados – Estudo experimental em coelhos

Alex de Lima Santos¹ Camila Gonzaga da Silva² Leticia Siqueira de Sá Barreto²
 Marcel Jun Sugawara Tamaoki¹ Fernando Gonçalves de Almeida² Flavio Faloppa¹

¹Department of Orthopedics and Traumatology, Escola Paulista de Medicina, Universidade Federal de São Paulo, São Paulo, SP, Brazil

²Department of Surgery, Escola Paulista de Medicina, Universidade Federal de São Paulo, SP, Brazil

Address for correspondence Alex de Lima Santos, Elbow and Shoulder Surgeon and PhD of the Escola Paulista de Medicina, Universidade Federal de São Paulo, Departamento de Ortopedia e Traumatologia, Escola Paulista de Medicina, UNIFESP, São Paulo, Brasil (e-mail: alexdels@gmail.com).

Rev Bras Ortop 2022;57(6):992–1000.

Abstract

Objective Semiquantitative and automated measurement of nuclear material removal and cell infiltration in decellularized tendon scaffolds (DTSs).

Method 16 pure New Zealand rabbits were used, and the gastrocnemius muscle tendon was collected bilaterally from half of these animals (16 tendons collected); 4 were kept as control and 12 were submitted to the decellularization protocol (DTS). Eight of the DTSs were used as an in vivo implant in the experimental rotator cuff tear (RCT) model, and the rest, as well as the controls, were used in the semiquantitative and automated evaluation of nuclear material removal. The eight additional rabbits were used to make the experimental model of RCT and subsequent evaluation of cellular infiltration after 2 or 8 weeks, within the DTS.

Results The semiquantitative and automated analysis used demonstrated a removal of 79% of nuclear material ($p < 0.001$ and power $> 99\%$) and a decrease of 88% ($p < 0.001$ and power $> 99\%$) in the area occupied by nuclear material after the decellularization protocol. On cell infiltration in DTS, an increase of 256% ($p < 0.001$ and power $> 99\%$) in the number of cells within the DTS was observed in the comparison between 2 and 8 weeks postoperatively.

Keywords

- ▶ tendons
- ▶ tissue engineering
- ▶ tissue scaffolds
- ▶ extracellular matrix
- ▶ regenerative medicine

Study developed at Escola Paulista de Medicina da Universidade Federal de São Paulo, São Paulo, SP, Brazil

received
October 30, 2020
accepted
June 25, 2021
published online
December 20, 2021

DOI <https://doi.org/10.1055/s-0041-1739174>.
ISSN 0102-3616.

© 2021. Sociedade Brasileira de Ortopedia e Traumatologia. All rights reserved.

This is an open access article published by Thieme under the terms of the Creative Commons Attribution-NonDerivative-NonCommercial-License, permitting copying and reproduction so long as the original work is given appropriate credit. Contents may not be used for commercial purposes, or adapted, remixed, transformed or built upon. (<https://creativecommons.org/licenses/by-nc-nd/4.0/>)

Thieme Revinter Publicações Ltda., Rua do Matoso 170, Rio de Janeiro, RJ, CEP 20270-135, Brazil

Conclusion The proposed semiquantitative and automated measurement method was able to objectively measure the removal of nuclear material and cell infiltration in DTS.

Resumo

Objetivo Mensuração semiquantitativa e automatizada da remoção de material nuclear e da infiltração celular em scaffolds tendinosos descelularizados (STDs).

Método Foram utilizados 16 coelhos Nova Zelândia puros, sendo o tendão do músculo gastrocnêmio coletado bilateralmente de metade destes animais (16 tendões coletados); 4 foram mantidos como controle e 12 foram submetidos ao protocolo de descelularização (STD). Dos STDs, 8 foram utilizados como implante in vivo no modelo experimental de lesão do manguito rotador (LMR) e os restantes, assim como os controles, foram utilizados na avaliação semiquantitativa e automatizada da remoção de material nuclear. Os oito coelhos adicionais foram utilizados na confecção do modelo experimental de LMR e posterior avaliação da infiltração celular após 2 ou 8 semanas, dentro do STD.

Resultados A análise semiquantitativa e automatizada utilizada demonstrou uma remoção de 79% do material nuclear ($p < 0,001$ e poder $> 99\%$) e uma diminuição de 88% ($p < 0,001$ e poder $> 99\%$) na área ocupada por material nuclear após o protocolo de descelularização. Sobre a infiltração celular no STD, foi observado um aumento de 256% ($p < 0,001$ e poder $> 99\%$) no número de células dentro do STD na comparação entre 2 e 8 semanas de pós-operatório.

Conclusão O método de mensuração semiquantitativo e automatizado proposto foi capaz de mensurar objetivamente a remoção de material nuclear e a infiltração celular no STD.

Palavras-chave

- ▶ tendões
- ▶ engenharia tecidual
- ▶ tecidos suporte
- ▶ matriz extracelular
- ▶ medicina regenerativa

Introduction

Rotator Cuff Tear (RCT) is a frequent cause of shoulder pain and may present clinically with a wide diversity of symptoms, with pain, weakness, and movement limitation being the most frequent.¹ Regarding its treatment, there are currently conservative or surgical options,² and their choice is performed according to the following criteria: (i) characteristics of the patient, (ii) morphology of the lesion, and (iii) main complaints.³ In the morphological evaluation, massive lesions are related to inferior postoperative outcomes than small.⁴

Seeking to optimize the results of surgical treatment of RCT with great retraction, there is a strong tendency to use tendon substitutes, whether decellularized or not.⁵ Conceptually, the tendon substitute is a tissue similar to the tendon and should perform its function when implanted in vivo.⁶ To be considered ideal, it must present the following characteristics: (a) structure in three dimensions with high porosity; (b) minimal cellular material, seeking to avoid inflammatory response; (c) cytocompatibility; and (d) biomechanical properties suitable to support the mechanical needs of rehabilitation up to complete cell infiltration and healing.^{7,8}

Tendon substitutes are commonly known as grafts; however, recently, the concept of scaffold has been widespread. Scaffolds are tissues that must allow cell infiltration and replication within their structure⁹ and can be used as grafts when applied in vivo. They can be classified, according to

their origin and composition, as synthetic or biological. Synthetics are industrialized polymers and present results with great variability according to the chosen material, function, and technique performed.^{10,11}

Regarding biological substitutes, they are subdivided according to their origin into autogenous, allogeneous and xenogeneous.^{7,12} Autogenous grafts are the gold standard; however, their low availability is the main obstacle to their use.⁷ Xenogeneous and allogeneous grafts, on the other hand, present, as adversity, uncontrolled inflammatory response and unsatisfactory tissue integration. Seeking to optimize the inflammatory response, to facilitate tissue integration, and to maximize the availability of biological substitutes, there is a strong tendency for its processing through decellularization.^{13,14} Decellularization is a processing that must combine physical, chemical, and enzymatic techniques and has the ability to remove cellular material.¹⁵⁻¹⁷

A decellularized tendinous scaffold (DTS) was recently evaluated in a Brazilian experimental study and presented maintenance of the main biomechanical properties and substantial removal of nuclear material, besides allowing cell infiltration.¹⁸ Regarding the removal of nuclear material and cell infiltration, the literature usually recommends descriptive analyses,^{13,15,19,20} and quantitative evaluation²¹ is one of the recent possibilities to optimize the validity of this evaluation.

Thus, in the search for alternatives to measure cell infiltration or removal, the present study proposes to evaluate

the hypothesis that the semiquantitative and automated methodology presented can perform the measurements proposed in DTSs.

Method

Experimental Design

Sixteen male rabbits (Pure New Zealand Rabbit, Granja RG-PR, Suzano, SP, Brazil) weighing between 3 and 3.5kg, maintained at the Center for the Development of Experimental Models for Medicine and Biology (CEDEME, in the Portuguese acronym) were used. The animals used were part of the validation of the previously published decellularization process,¹⁸ and the present study refers to the presentation of a new methodology for semiquantitative and automated measurement of nuclear material removal and cell infiltration of these same specimens. During the experiments, the animals remained in individual cages, with a light/dark cycle of 12/12hrs, food and water ad libitum.²² The study was approved by the Ethics Committee on the Use of Animals (CEUA527208916), followed the guidelines proposed by the ARRIVE guideline,²³ and received support from the National Council for Scientific and Technological Development (CNPq, in the Portuguese acronym) (311237/2018–5).

To perform the experiments, the animals were divided into two different designs: in the first, the gastrocnemius muscle tendon was collected, and the DTS was prepared. A total of 16 tendons of the gastrocnemius muscle (corresponding to 8 animals) were collected, 12 of which were submitted to the decellularization protocol (DTS), and the

other 4 were maintained as controls. Eight DTSs were inserted in the experimental model *in vivo* and four were used in the histological evaluation (→ **Figure 1**). The remaining eight animals (→ **Figure 1**) were used in the experimental models of RCT, as shown below.

Preparation of Scaffold from Decellularized Tendon

The decellularization protocol used for DTS production, which has been published and validated previously,¹⁸ presents the following steps: the gastrocnemius muscle tendons were washed with phosphate buffered saline (PBS) solution containing 1% antibiotic (penicillin-streptomycin solution; Sigma-Aldrich, St. Louis, MO, USA) for removal of surface residues and of the decellularizing agent used in the previous stage.

The remainder of the protocol included maintenance of the specimens in constant agitation (MaxQ4000; Thermo Scientific, Waltham, MA, USA) and subsequent exchanges of the following decellularizing agents: aprotinin (Sigma-Aldrich St. Louis, MO, USA), ethylenediaminetetraacetic Acid (EDTA) (Sigma-Aldrich, St. Louis, MO, USA), sodium sulfate (SDS) (Invitrogen, Carlsbad, CA, USA), and t-octylphenoxypolyethoxyethanol (Triton X-100) (Affymetrix, Maumme, Ohio, USA).

In vivo Experimental Model of Rotator Cuff Injury

For the preparation of the experimental RCT model, the animal was submitted to the following anesthesia and analgesia protocol: initial analgesia and preoperative antibiotic therapy with tramadol (5 mg/kg) and terramycin (50 mg/kg); after 30 minutes, anesthesia was started with ketamine (50

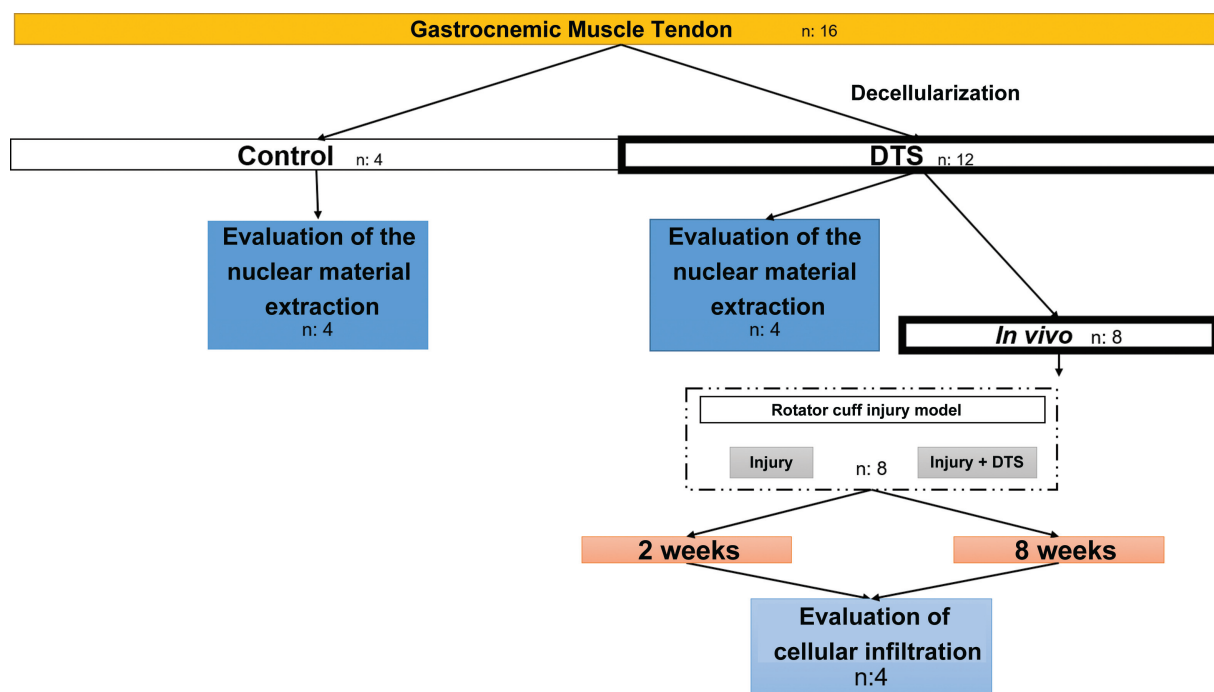


Fig. 1 Experimental design. General organization chart for division of the groups presenting the 12 decellularized tendon scaffolds (DTSs) produced, the 8 submitted to implant and subsequent evaluation of *in vivo* cellular infiltration. In the same image, are also presented the four DTS and four controls submitted to evaluation of the removal of nuclear material.

mg/kg) and xylazine (10 mg/kg). In the postoperative analgesia, the animal was maintained with meloxicam (0.5 mg/kg) and tramadol (5 mg/kg) until completing the 3rd postoperative day, and these medications were administered in case of pain or discomfort after this period. Evaluations regarding stress, discomfort, and pain were performed daily at CEDEME.

After anesthesia, the animals were positioned in the supine position and submitted to bilateral glenohumeral joint trichotomy, asepsis, and antiseptis. Thus, both front paws were submitted to the RCT protocol and then allocated into the "Injury" or "Injury + DTS" groups. For allocation, simple randomization was performed, so that one of the paws was used as the contralateral control.

For the injury protocol, an anterolateral pathway was performed in the shoulder, with exposure and dissection of the deltoid muscle between its anterior and middle sections (►Figure 1a). After dissection of the interval and exposure of the subscapularis tendon (►Figure 2b), a lesion parallel to the tendon fibers was performed throughout their extension (►Figure 2c), without disinsertion in the osteotendinous junction²⁴ (►Figure 2d). After the injury, the DTS was positioned in one of the paws, exactly on the site of the experimental lesion, and had its extremities fixed with nylon (Nylon 4-0; Shalon, Alto da Boa Vista, GO, Brazil). The contralateral was submitted only to the marking of the lesion. In this experimental model, we limit the

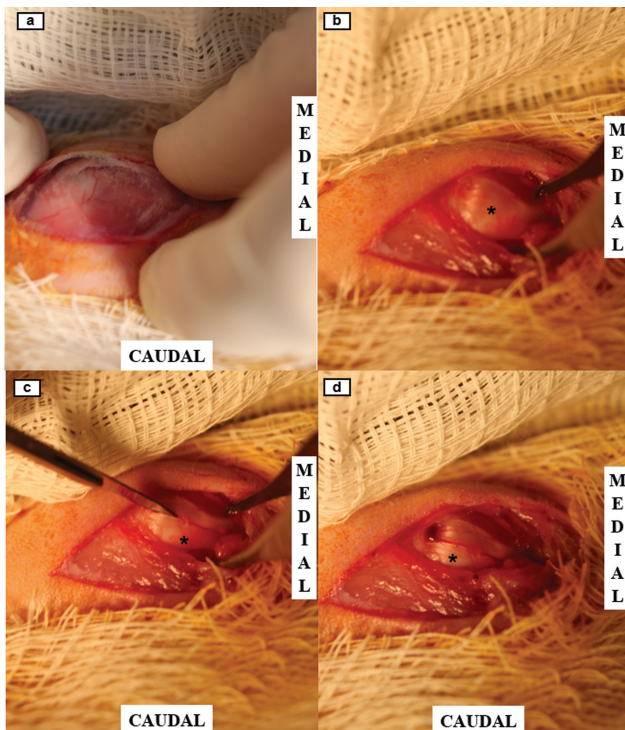


Fig. 2 Experimental Rotator Cuff Tear (RCT) protocol. Demonstration of the anterolateral approach and deltoid exposure; (b) Exposure of the anterior part of the rotator cuff, the subscapularis muscle tendon; (c) Performance of RCT with cold blade, throughout the tendon, and without disinsertion of the rotator cuff; (d) Final aspect of the experimental RCT protocol. Asterisk (*) identification of the rotator cuff tendon.

biomechanical requirements to which the DTS would be subjected, thus ensuring that there would be no failures in the fixation of the DTS to the rotator cuff. However, the results obtained would be limited to the inflammatory response and tissue integration between the DTS and the rotator cuff.

The animals were again randomized in relation to postoperative time (2 or 8 weeks postoperatively) and submitted to painless induced death, with an overdose of anesthetics (ketamine 200mg/kg + xylazine 40 mg/kg and tramadol 10 mg/kg). Then, the previously marked region was collected, necessarily including the rotator cuff throughout the lesion and the DTS.

Preparation and Coloring with Hematoxylin and Eosin

The central part of the DTS ($n=4$), of the control ($n=4$), and the material resulting from the *in vivo* analysis (Injury [$n=8$] and Lesion + Scaffold [$n=8$]) were prepared through the following protocol: fixation in 10% formaldehyde, dehydrated with ethyl alcohol, diaphanized by xylol, and impregnated with liquid paraffin. Manual inclusion and positioning of the microtome blocks was then performed for cuts with a thickness of 4 μm and a distance of 50 μm . Prior to staining with hematoxylin and eosin (H&E), the sections were deparalinated with xylol, hydrated with ethyl alcohol concentrations and immersed in distilled water. For staining with the H&E technique, immersion in hematoxylin solution, the sections were washed in running water and dehydrated with ethyl alcohol until they were colored with eosin. The H&E-colored histological slides were evaluated using the Olympus IX 81 optical

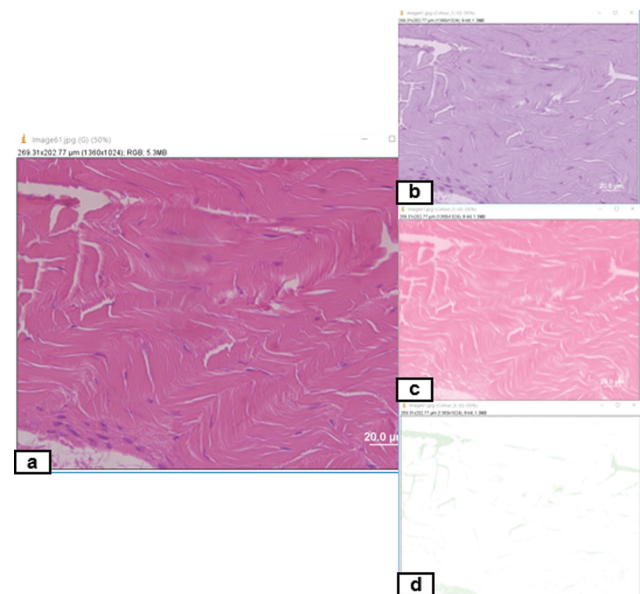


Fig. 3 Decomposition of H&E-colored images for semiquantitative and automated measurement. (a) Original photograph of the histological cut in H&E staining; (b) Photograph from the decomposition with enhancement of the purplish color (eosin enhancement); (c) Photograph from decomposition with enhancement of rosy staining (hematoxylin enhancement); (d) Photograph from decomposition to assess the quality of decomposition.

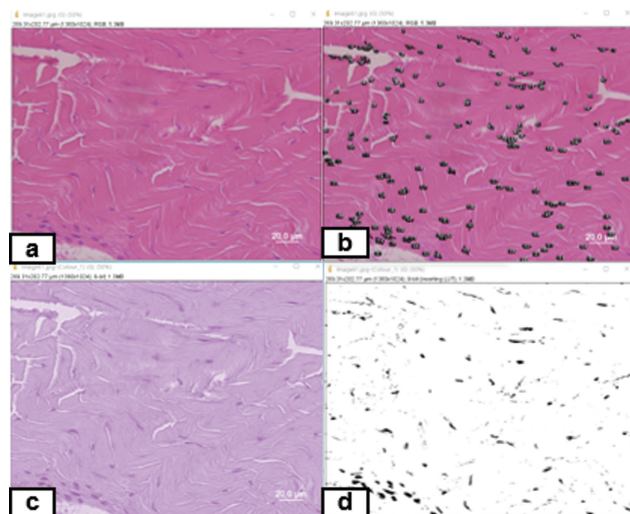


Fig. 4 Semiquantitative and automated measurement method (a) Original image in H&E; (b) Original H&E-colored image with representation of the nuclear structures accounted; (c) Image from decomposition with enhancement of purplish staining (eosin enhancement); (d) Image demonstrating the result of conversion to binary format.

microscope (Olympus Corporation, Shinjuku-ku, Tokyo, Japan) with fluorescence, while the images were captured by an Olympus DP72 camera (Olympus Corporation, Shinjuku-ku, Tokyo, Japan) coupled to the microscope.

Semiquantitative and Automated Analysis of Nuclear Material Removal and Cellular Infiltration

The analysis of nuclear material, be it removal or cell invasion, was performed using a semiquantitative methodology,²¹ with an automated method. In this methodology, the removal of nuclear material was classified as: complete (100%), substantial (99–70%), moderate (69–50%), minimum (49–30%) and no change (< 30%).⁶ For the semiquantitative and automated analysis of nuclear material removal, the slides referring to four DTS and four controls were performed and in a way of evaluate cell infiltration, the same method was used to quantified the number of nucleus in four Lesions + DTS with 2 weeks and another four Lesion + DTS with 8 weeks postoperatively.

To measure cell infiltration, we applied the methodology only in the region corresponding to the DTS. For counting, 10 random fields were photographed clockwise from superior to lower with an increase of 400x, thus totaling 40 control photographs, 40 of DTS, 40 of the Lesion + DTS group with 2 weeks, and 40 of the Lesion + DTS group with 8 weeks postoperatively.

The photographs were inserted in Image J software (Image J 1.53e; National Institutes of Health, Bethesda MA, USA), and the scale was adjusted in the first image evaluated. To start the counting, the color was decombed using the “colour deconvolution - H&E2” plugin (→Figure 3) and only the image with eosin color enhancement (→Figures 3B and →Figure 4C) was selected, which highlights the nuclear material. The figures

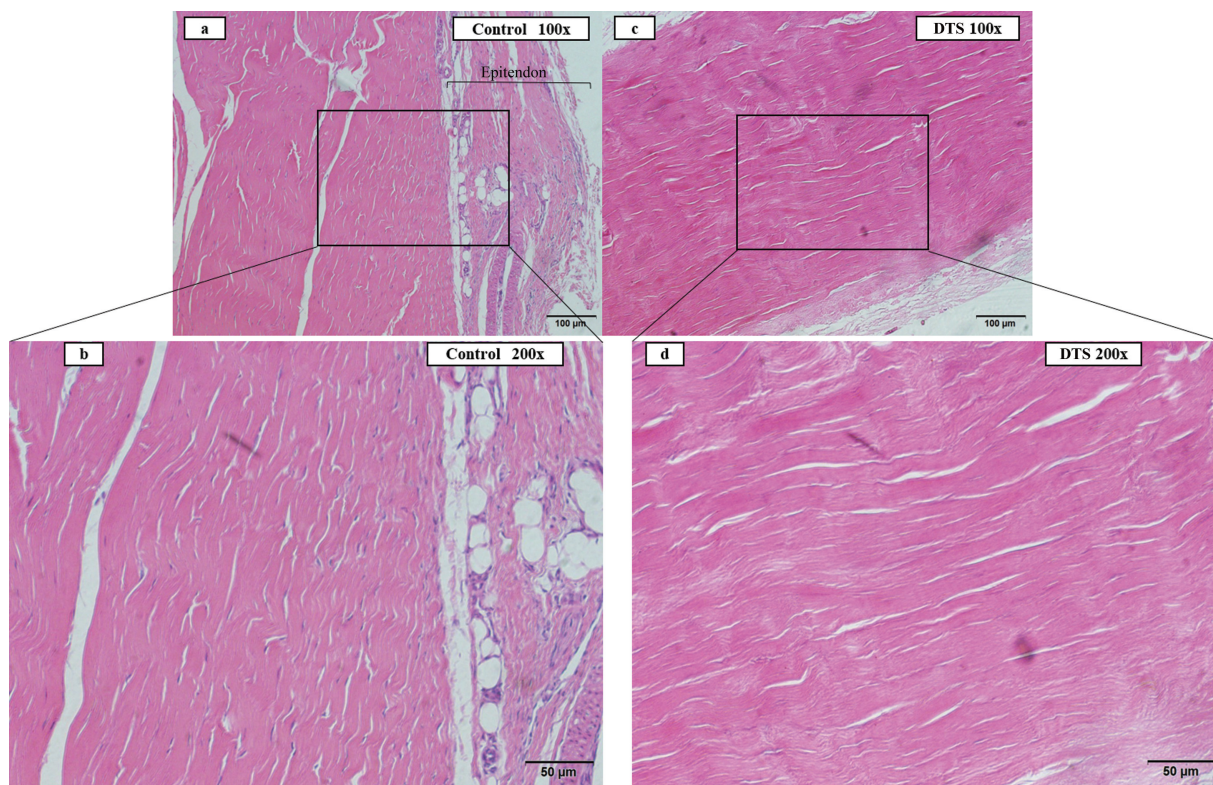


Fig. 5 Control and DTS – presentation with H&E slices (a) Image in 100x increase presenting the control and its respective structures; (b) an increased image of 200x clearly representing nuclear structures; (c) 100x increased image presenting the DTS with maintenance of the basic architecture and parallelism of tendon fibers; (d) Images with an increase of 200x presenting the absence of nuclear structures with a typical aspect to that found in the control.

were then manually adjusted in the topic image - adjust - threshold and then converted to the binary format (process - binary - convert to mask - make binary) (► **Figure 4d**). As a final step, automated counting was performed using the analyze function - analyze particles (size 1-100µm²; circularity 0.00-1.00; outlines; exclude on edges; include holes) (► **Figure 4b**). The software provided the following results at the end of the process: total nucleus count, total nucleus area, average area of the nucleus, and percentage of area of each photograph occupied by the nucleus.

Statistical analysis

Using the available literature,²¹ we found a similar decellularization protocol, with removal of 97.5% (±2%) of nuclear material. Applying this difference between the groups, through the two-sample t test for mean differences, considering an alpha of 0.05 and a power of 95%, the minimum number of specimens per group was 2. For statistical difference evaluation, the Wilcoxon-Mann-Whitney nonparametric test was chosen using SAS Studio software (SAS 3.8 Basic Edition; SAS Institute, Cary, NC, USA), and p < 0.05 is presumed as a statistically significant difference. As a mechanism to evaluate the results obtained, we also chose to evaluate in a post hoc way (satterthwaite t-test) the statistical power of the results found, using SAS Studio software (SAS 3.8 Basic Edition; SAS Institute, Cary, NC, USA). Microsoft Excel for Office 365 (Microsoft Corporation, Redmond, WA, USA) was used to assemble the tables (descriptive presentation) and prepare the graphs.

Results

Measurement of Decellularization by Semiquantitative and Automated Method

A substantial decrease in nuclear material was observed (► **Figure 6**), since ~ 79% (p < 0.0001 and statistical power > 99%) of this material was removed during decellularization (► **Figure 6** and ► **Table 1**). Also in the semiquantitative analysis, we noticed a reduction of ~ 88% (p < 0.001 and statistical power > 99%) in the area occupied by nuclear structures after the decellularization protocol, confirming the substantial removal of nuclear material (► **Table 2**).

Measurement of Cellular Infiltration in DTS After Implant In Vivo

The DTSs were easily characterized, in macroscopic and histological vision, in the different postoperative moments (► **Figures 7** and **8**). Throughout the postoperative period, the DTS was in progressive integration with the rotator cuff, since it was possible to notice cellular infiltration still restricted to the peripheries of the DTS after 2 weeks, and a more comprehensive infiltration after 8 weeks postoperatively (► **Figure 8**).

In the automated measurement, the DTS presented an average of 50.45 cells, a number that remained stable after implantation in vivo and after 2 weeks postoperatively (p = 0.6081) and increased significantly to 148.67 cells

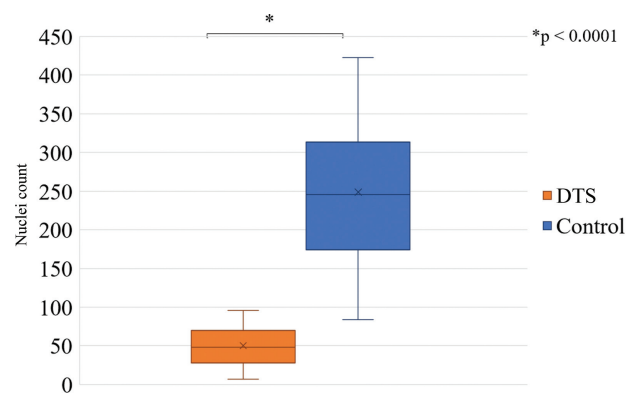


Fig. 6 Removal of nuclear material in the decellularization process - graphic representation Graph representative of the substantial decrease of nuclear material after the decellularization protocol, with statistical significance.

Table 1 Automated and semiquantitative nuclear material count

	Nucleus count (SD)	p-value
Control	248.85 (91.53)	< 0.0001
DTS	50.45 (24.35)	
RCT + DTS - 2 weeks PO	57.90 (50.49)	< 0.0001
RCT + DTS - 8 weeks PO	148.67 (82.29)	

Abbreviations: DTS, decellularized tendon scaffold; PO, postoperatively; SD, standard deviation.

Difference between control and DTS demonstrates substantial removal of nuclear material with statistical significance. Similarly, the increase in the number of nuclei over the postoperative period demonstrates progressive cellular infiltration in the DTS, with statistical significance.

Table 2 Automated and semiquantitative measurement of the area occupied by nuclear material

	Nucleus count (SD)	p-value
Control	2.628% (1.094%)	< 0.0001
DTS	0.293% (0.175%)	
RCT + DTS - 2 weeks PO	0.558% (0.552%)	< 0.0001
RCT + DTS - 8 weeks PO	1.795% (1.353%)	

Abbreviations: DTS, decellularized tendon scaffold; PO, postoperatively; SD, standard deviation.

Difference in the area occupied by nuclear material between control and DTS demonstrates substantial removal of nuclear material with statistical significance. Similarly, the increase of this area over the postoperative period demonstrates progressive cellular infiltration in the DTS, with statistical significance.

(p < 0.001 and power > 99%) after 8 weeks postoperatively (► **Table 1** and ► **Figure 9**).

In the measurement of the area, there was a similar increase: the DTS presented 0.175% of the area occupied by nuclei; after 2 weeks, this area remained stable

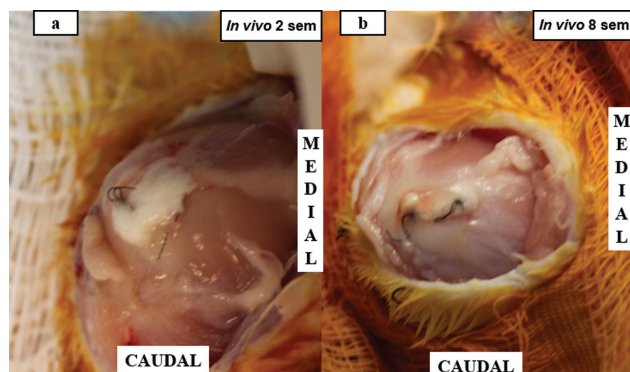


Fig. 7 In vivo macroscopy of the integration between the DTS and the rotator cuff (a). Macroscopic aspect of the integration between the DTS after 2 weeks postoperatively, demonstrating initial integration and connective tissue between the DTS and the rotator cuff. (b). Macroscopic aspect of integration between DTS after 8 weeks postoperatively, demonstrating integration in the most advanced phase between the DTS and the rotator cuff. Sem: week.

($p=0.1611$), and it increased to 1.795% ($p < 0.001$ and statistical power $> 99\%$) 8 weeks postoperatively (► **Table 2**).

Discussion

The main findings of the present study are the presentation of an innovative, semiquantitative and automated method

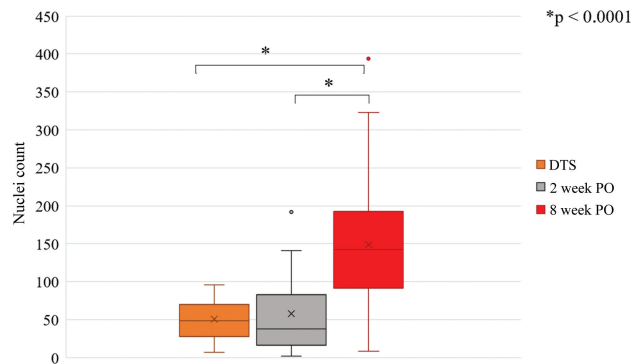


Fig. 9 Progressive cellular infiltration in DTS. Graphic representation of progressive cellular infiltration in DTS, demonstrating a DTS with approximately 50 cells, a number that remained constant after 2 weeks and increased significantly to 150 cells after 8 weeks postoperatively.

for measuring the removal of nuclear material and cellular infiltration in decellularized tissues produced in Brazil and that are possible to be evaluated for tendon replacement in the most diverse lesions, possibly in RCT with great retraction.

The search for tendon substitutes is not recent, since the problem related to RCT with great retraction is ancient. Currently, the use of autologous material is presented as the gold standard;^{25,26} however, the limitations related to its

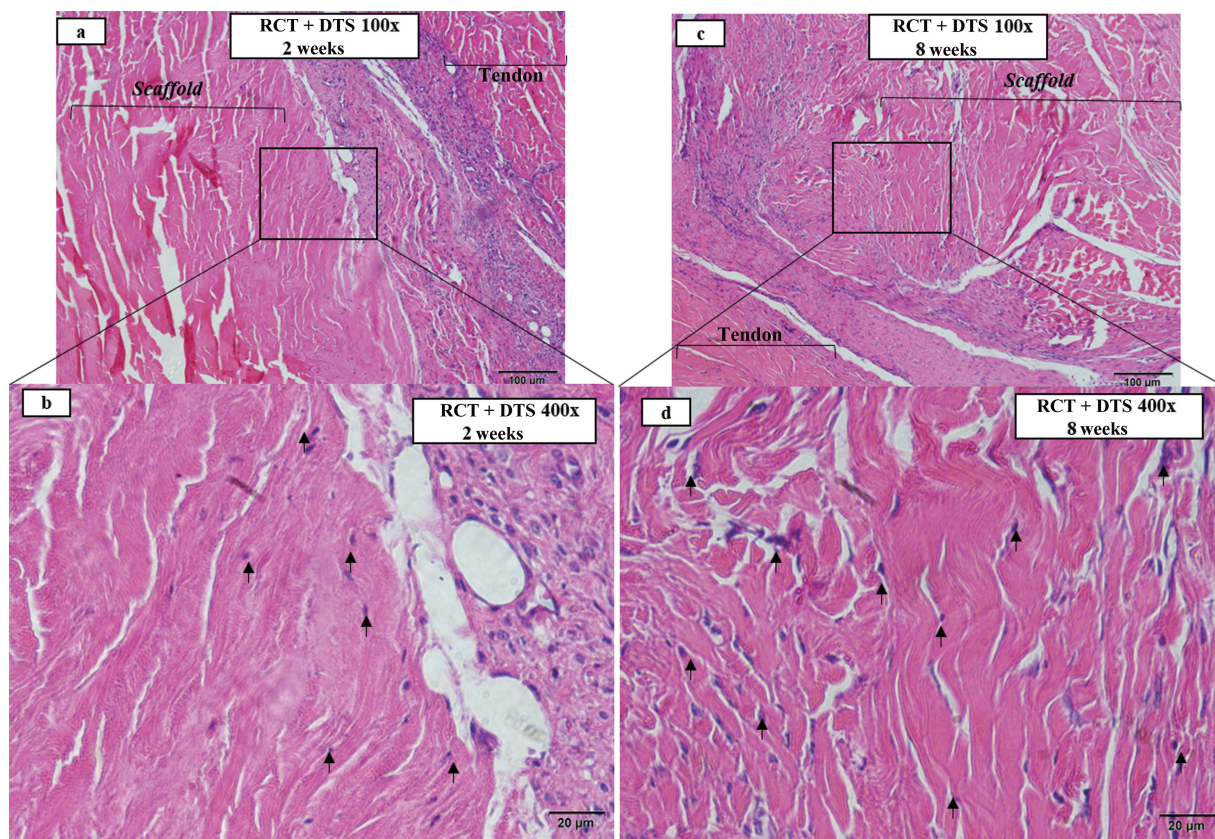


Fig. 8 In vivo tissue integration - H&E representation (a) H&E image with 100x increase clearly demonstrating rotator cuff tendon and DTS; (b) H&E image with 400x increase demonstrating cell infiltration restricted to the periphery of the DTS; (c) H&E image with 100x increase clearly demonstrating DTS and tendon tissue; (d) H&E imaging with 400x increase demonstrating cellular infiltration in all DTS regions. Marking on arrows demonstrating cellular infiltration in images c and d.

use (biomechanical inability to replace the original tissue) and collection (morbidity at the donor site and limited availability) motivate the search for new alternatives.

Considering these limitations, it is essential to search for alternative tissues that can perform functions similar to those of the tendon, and decellularization is the most promising method.^{16,27,28} In this sense, the measurement of the reduction of nuclear material in the processing and favoring of cellular infiltration after in vivo implantation are important objectives to be used in subsequent studies.

These studies should seek to develop an ideal tendon substitute, overcoming the current limitations of biologicals; thus, it should be a product with acceptable biocompatibility, no risk for disease transmission, low risk for chronic inflammatory response, and storage capacity for long periods.

The main limitations of the present study are related to the small number of specimens evaluated, the absence of additional evaluations, such as the objective measurement of DNA and remaining collagen, and the characteristics of the experimental model. The experimental lesion used does not reproduce the conventional lesions of the rotator cuff; however, it favors tendon healing and tissue integration in the DTS/tendon interface.

As a strong point of the present study, the use of DTS is promising in Brazil, since Brazilian legislation does not allow the commercialization of some tissues with an allogeneous origin used in other countries. In this perspective, the standardization of decellularization in a center for human tissue management may provide a viable alternative for future studies of patients with RCT.

Conclusion

The proposed semiquantitative and automated measurement method was able to objectively measure the removal of nuclear material and cellular infiltration in the scaffold.

Financing Support

The present study was funded by the National Council for Scientific and Technological Development (CNPq) – process number 311237/2018-5.

Conflict of Interests

The authors have no conflict of interests to declare.

References

- Assunção JH, Malavolta EA, Domingues VR, Gracitelli MEC, Ferreira Neto AA. Avaliação dos desfechos no tratamento da rotura do manguito rotador: o que usamos no Brasil? *Rev Bras Ortop* 2017; 52(05):561–568
- Godinho GG, França FO, Freitas JMA, et al. Avaliação da integridade anatômica por exame de ultrassom e funcional pelo índice de Constant & Murley do manguito rotador após reparo artroscópico. *Rev Bras Ortop* 2010;45(02):174–180
- Vieira FA, Olawa PJ, Belangero PS, Arliani GG, Figueiredo EA, Ejnisman B. Lesão do manguito rotador: tratamento e reabilitação. Perspectivas e tendências atuais. *Rev Bras Ortop* 2015;50(06):647–651
- Godinho AC, Santos FML, Donato Neto FP, Silva PVNP, Fonseca Júnior RD. Evaluation of the functional outcomes of arthroscopic surgical treatment of complete rotator cuff lesion with minimum follow-up of 10 years. *Rev Bras Ortop* (Sao Paulo) 2020;55(05):579–584
- Bailey JR, Kim C, Alentorn-Geli E, et al. Rotator Cuff Matrix Augmentation and Interposition: A Systematic Review and Meta-analysis. *Am J Sports Med* 2019;47(06):1496–1506
- Liu GM, Pan J, Zhang Y, et al. Bridging Repair of Large Rotator Cuff Tears Using a Multilayer Decellularized Tendon Slices Graft in a Rabbit Model. *Arthroscopy* 2018;34(09):2569–2578
- Cheng CW, Solorio LD, Alsberg E. Decellularized tissue and cell-derived extracellular matrices as scaffolds for orthopaedic tissue engineering. *Biotechnol Adv* 2014;32(02):462–484
- Whitlock PW, Smith TL, Poehling GG, Shilt JS, Van Dyke M. A naturally derived, cytocompatible, and architecturally optimized scaffold for tendon and ligament regeneration. *Biomaterials* 2007;28(29):4321–4329
- Langer R, Vacanti JP. Tissue engineering. *Science* 1993;260(5110):920–926
- Ventura A, Terzaghi C, Legnani C, Borgo E, Albisetti W. Synthetic grafts for anterior cruciate ligament rupture: 19-year outcome study. *Knee* 2010;17(02):108–113
- Shepherd HM, Lam PH, Murrell GAC. Synthetic Patch Rotator Cuff Repair: A 10-year Follow-Up. *Shoulder Elbow* 2014;6(01):35–39
- Andreassi A, Bilenchi R, Biagioli M, D'Aniello C. Classification and pathophysiology of skin grafts. *Clin Dermatol* 2005;23(04):332–337
- Xing S, Liu C, Xu B, Chen J, Yin D, Zhang C. Effects of various decellularization methods on histological and biomechanical properties of rabbit tendons. *Exp Ther Med* 2014;8(02):628–634
- Livesey SA, Herndon DN, Hollyoak MA, Atkinson YH, Nag A. Transplanted acellular allograft dermal matrix. Potential as a template for the reconstruction of viable dermis. *Transplantation* 1995;60(01):1–9
- Lovati AB, Bottagisio M, Moretti M. Decellularized and Engineered Tendons as Biological Substitutes: A Critical Review. *Stem Cells Int* 2016;2016:7276150
- Crapo PM, Gilbert TW, Badylak SF. An overview of tissue and whole organ decellularization processes. *Biomaterials* 2011;32(12):3233–3243
- Schulze-Tanzil G, Al-Sadi O, Ertel W, Lohan A. Decellularized tendon extracellular matrix—a valuable approach for tendon reconstruction? *Cells* 2012;1(04):1010–1028
- de Lima Santos A, da Silva CG, de Sá Barreto LS, et al. A new decellularized tendon scaffold for rotator cuff tears - evaluation in rabbits. *BMC Musculoskelet Disord* 2020;21(01):689
- Whitlock PW, Seyler TM, Parks GD, et al. A novel process for optimizing musculoskeletal allograft tissue to improve safety, ultrastructural properties, and cell infiltration. *J Bone Joint Surg Am* 2012;94(16):1458–1467
- Netto ADS, Antebi U, Morais CE, Sementilli L, Severino NR, Cury RPL. Evaluation of Histological Properties of Human Meniscal Grafts Stored in a Tissue Bank. *Rev Bras Ortop* (Sao Paulo) 2020;55(06):778–782
- Roth SP, Glauche SM, Plenge A, Erbe I, Heller S, Burk J. Automated freeze-thaw cycles for decellularization of tendon tissue - a pilot study. *BMC Biotechnol* 2017;17(01):13
- de Lima Santos A, Silva CGD, de Sá Barreto LS, et al. Biomechanical evaluation of tendon regeneration with adipose-derived stem cell. *J Orthop Res* 2019;37(06):1281–1286
- Percie du Sert N, Ahluwalia A, Alam S, et al. Reporting animal research: Explanation and elaboration for the ARRIVE guidelines 2.0. *PLoS Biol* 2020;18(07):e3000411
- Grumet RC, Hadley S, Diltz MV, Lee TQ, Gupta R. Development of a new model for rotator cuff pathology: the rabbit subscapularis muscle. *Acta Orthop* 2009;80(01):97–103

- 25 Grau HR. The artificial tendon: an experimental study. *Plast Reconstr Surg Transplant Bull* 1958;22(06):562-566
- 26 White WL. Tendon grafts: a consideration of their source, procurement and suitability. *Surg Clin North Am* 1960;40(02):403-413
- 27 Cartmell JS, Dunn MG. Effect of chemical treatments on tendon cellularity and mechanical properties. *J Biomed Mater Res* 2000;49(01):134-140
- 28 Youngstrom DW, Barrett JG. Engineering Tendon: Scaffolds, Bioreactors, and Models of Regeneration. *Stem Cells Int* 2016;2016:3919030